Article

Androgynous Porphyrins. Silver(II) Quinoxalinoporphyrins Act as Both Good Electron Donors and Acceptors

Shunichi Fukuzumi, Kei Ohkubo, Weihua Zhu, Maxine Sintic, Tony Khoury, Paul J. Sintic, Wenbo E, Zhongping Ou, Maxwell J. Crossley, and Karl M. Kadish

J. Am. Chem. Soc., **2008**, 130 (29), 9451-9458 • DOI: 10.1021/ja801318b • Publication Date (Web): 28 June 2008

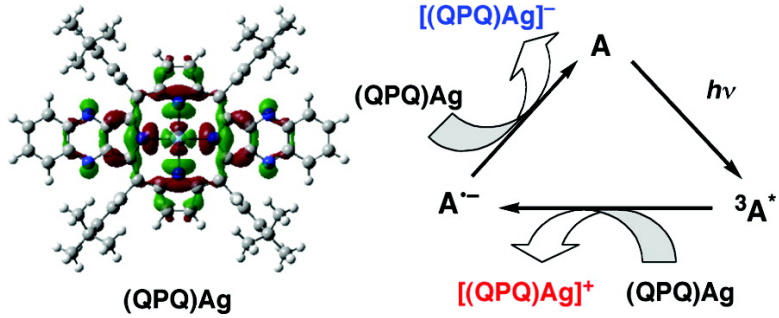

More About This Article

Additional resources and features associated with this article are available within the HTML version:

- Supporting Information
- Access to high resolution figures
- Links to articles and content related to this article
- Copyright permission to reproduce figures and/or text from this article

View the Full Text HTML

J|A|C|S
ARTICLES

Published on Web 06/28/2008

Androgynous Porphyrins. Silver(II) Quinoxalinoporphyrins Act as Both Good Electron Donors and Acceptors

Shunichi Fukuzumi,*,† Kei Ohkubo,† Weihua Zhu,‡ Maxine Sintic,§ Tony Khoury,§ Paul J. Sintic,§ Wenbo E,‡ Zhongping Ou,‡ Maxwell J. Crossley,*,§ and Karl M. Kadish*,‡

Department of Material and Life Science, Graduate School of Engineering, Osaka University, SORST, Japan Science and Technology Agency (JST), Suita, Osaka 565-0871, Japan, Department of Chemistry, University of Houston, Houston, Texas 77204-5003, and School of Chemistry, The University of Sydney, NSW 2006, Australia

Received February 22, 2008; E-mail: fukuzumi@chem.eng.osaka-u.ac.jp; m.crossley@chem.usyd.edu.au; kkadish@uh.edu

Abstract: The metal-centered and macrocycle-centered electron-transfer oxidations and reductions of silver(II) porphyrins were characterized in nonaqueous media by electrochemistry, UV−vis spectroelectrochemistry, EPR spectroscopy, and DFT calculations. The investigated compounds are {5,10,15,20-tetrakis(3,5-di-*tert*-butylphenyl)porphyrinato}silver(II), {5,10,15,20-tetrakis(3,5-di-*tert*-butylphenyl)quinoxalino[2,3-*b*′]porphyrinato}silver(II), {5,10,15,20-tetrakis(3,5-di-*tert*-butylphenyl)bisquinoxalino[2,3-*b*′:7,8-*b*′′]porphyrinato}silver(II), and {5,10,15,20-tetrakis(3,5-di-*tert*-butylphenyl)bisquinoxalino[2,3-*b*′:12,13-*b*′′]porphyrinato}silver(II). The first one-electron oxidation and first one-electron reduction both occur at the metal center to produce stable compounds with Ag(III) or Ag(I) metal oxidation states, irrespective of the type of porphyrin ligand. The electrochemical HOMO−LUMO gap, determined by the difference in the first oxidation and first reduction potentials, decreases by introduction of quinoxaline groups fused to the Ag(II) porphyrin macrocycle. This provides a unique androgynous character to Ag(II) quinoxalinoporphyrins that enables them to act as both good electron donors and good electron acceptors, something not previously observed in other metalloporphyrin complexes. The second one-electron oxidation and second one-electron reduction of the compounds both occur at the porphyrin macrocycle to produce Ag(III) porphyrin π-radical cations and Ag(I) porphyrin π-radical anions, respectively. The macrocycle-centered oxidation potentials of each quinoxalinoporphyrin are shifted in a negative direction, while the macrocycle-centered reduction potentials are shifted in a positive direction as compared to the same electrode reactions of the porphyrin without the fused quinoxaline ring(s). Both potential shifts are due to a stabilization of the radical cations and radical anions by π-extension of the porphyrin macrocycle after fusion of one or two quinoxaline moieties at the β-pyrrolic positions of the macrocycle. Introduction of quinoxaline groups fused to the Ag(II) porphyrin macrocycle provides a unique androgynous character to Ag(II) quinoxalinoporphyrins that enables them to act as both good electron donors and good electron acceptors.

Introduction

Porphyrins contain an extensively conjugated two-dimensional π-system, which makes them suitable for efficient electron transfer, as the uptake or release of electrons results in minimal structural and solvation change upon electron transfer.[1] Porphyrin macrocyclic ligands can tightly bind numerous metal ions, many of which are redox active and can thus undergo one or more metal-centered reductions or oxidations.[2] Metalloporphyrins have normally been used as good electron donors, in particular for photoinduced electron transfer reactions because the oxidation potentials of metalloporphyrins are lower than those of free-base porphyrins.[3–6] When metalloporphyrins act as good electron donors, they are not able to act as good electron acceptors because the HOMO−LUMO gap of most metalloporphyrins is generally constant for macrocycle-centered reactions,

† Osaka University, SORST, JST.
‡ University of Houston.
§ University of Sydney.

(1) Fukuzumi, S. In *The Porphyrin Handbook*; Kadish, K. M., Smith, K. M., Guilard, R., Eds.; Academic Press: San Diego, CA, 2000; Vol. 8, pp 115−152.
(2) Kadish, K. M.; Van Caemelbecke, E.; Royal, G. In *The Porphyrin Handbook*; Kadish, K. M., Smith, K. M., Guilard, R., Eds.; Academic Press: San Diego, CA, 2000; Vol. 8; pp 1−114.
(3) (a) Wasielewski, M. R. *Chem. Rev.* **1992**, *92*, 435. (b) Wasielewski, M. R.; Wiederrecht, G. P.; Svec, W. A.; Niemczyk, M. P. *Sol. Energy Mater. Sol. Cells* **1995**, *38*, 127.
(4) (a) Gust, D.; Moore, T. A. In *The Porphyrin Handbook*; Kadish, K. M., Smith, K. M., Guilard, R., Eds.; Academic Press: San Diego, CA, 2000; Vol. 8, pp 153−190. (b) Gust, D.; Moore T. A.; Moore, A. L. In *Electron Transfer in Chemistry*; Balzani, V., Ed.; Wiley-VCH: Weinheim, Germany, 2001; Vol. 3, pp 272−336.
(5) Fukuzumi, S.; Imahori, H. In *Electron Transfer in Chemistry*; Balzani, V., Ed.; Wiley-VCH: Weinheim, Germany, 2001; Vol. 2, pp 927−975.
(6) Fukuzumi, S.; Guldi, D. M. In *Electron Transfer in Chemistry*; Balzani, V., Ed.; Wiley-VCH: Weinheim, Germany, 2001; Vol. 2, pp 270−337.

10.1021/ja801318b CCC: $40.75

and thus one observes either a facile oxidation or a facile reduction but not both for the same compound.[1–6]

Metal-centered reductions of metalloporphyrins generally occur at potentials more positive than for reduction at the conjugated macrocycle,[2] and when this occurs the porphyrin can act as a good electron acceptor, one example being Au(III) porphyrins,[7,8] which have frequently been used as electron acceptor components in linked donor−acceptor molecules.[9–14] However, the same Au(III) porphyrins will not act as good electron donors because the metal center cannot be further oxidized and electron abstraction from the conjugated macrocycle occurs only at very positive potentials,[7,8] far beyond what is needed for a good electron donor.

In contrast to Au(III) porphyrins, the Ag(II) complexes undergo both oxidation and reduction involving the metal center to produce Ag(III) and Ag(I) porphyrins before electron transfer reactions at the porphyrin macrocycle.[15–22] Like Cu(II) porphyrins, a d^9 configuration exists for the central metal ion of Ag(II) porphyrins, but the site of oxidation in the two series of related metal complexes is different in that the first one-electron oxidation of the Cu(II) porphyrins leads to a π-radical cation rather than generating a Cu(III) porphyrin with an unoxidized macrocyclic ring.[15,23–28] This is because its $d_{x^2-y^2}$ orbital energies are significantly lower than those of the related Ag(II) porphyrins having the same electronic configuration. Thus, $(TPP)Ag^{II}$ (TTP^{2-} = dianion of tetraphenylporphyrin) is a relatively good electron donor as indicated by its low oxidation potential (0.59 V vs SCE), but it is not a good electron acceptor because its reduction potential is too negative to act in this capacity (−1.01 V vs SCE).[29] On the other hand, introducing strongly electron-withdrawing groups such as NO_2 onto the four *meso*-phenyl substituents of the tetraphenylporphyrin molecule to give ((p-NO_2)TPP)Ag will lead to a positive shift of the reduction potential (to $E_{1/2} = -0.83$ V vs SCE in CH_2Cl_2), and the porphyrin then becomes a stronger electron acceptor; at the same time the compound becomes a weaker electron donor because its oxidation potential is also shifted positively, in this case to 0.78 V vs SCE[29] from the value of 0.59 V in the absence of the electron-withdrawing substituents.

The potentials for oxidation or reduction of a metalloporphyrin and the magnitude of the compound's HOMO−LUMO gap can also be modulated by fusing quinoxaline groups at the β-pyrrole positions of the porphyrin macrocycle in either a linear or corner fashion.[30,31] For example, the HOMO−LUMO gap of the doubly ring-annulated bisquinoxalinoporphyrin (QPQ)Zn is lowered to 1.90 eV as compared to its free-base analogue in the absence of the metal ion, $(QPQ)H_2$ (2.14 eV).[31] (QPQ)Zn can then act as a relatively good electron donor with its oxidation potential of 0.76 V, but it is still not a good electron acceptor because its reduction potential remains too negative, being −1.14 V vs SCE.[31]

In contrast to what happens in the case of the Zn(II) porphyrins, the introduction of quinoxaline groups fused to an Ag(II) porphyrin macrocycle will give derivatives that are both easier to reduce and easier to oxidize than the zinc quinoxalinoporphyrins, since in this case the electron additions and abstractions both occur at the metal center. This is described in the present article, where it is shown that Ag(II) quinoxalinoporphyrins have a unique androgynous character in that they can act as both good electron donors and good electron acceptors at the same time. The investigated compounds are shown in Chart 1 and were characterized in nonaqueous media by electrochemistry, UV−vis spectroelectrochemistry, and EPR spectroscopy. The unique androgynous character of Ag(II) quinoxalinoporphyrins is demonstrated in the photoinduced electron transfer reactions with a Zn(II) porphyrin and tetramethyl-*p*-benzoquinone, which afford both the oxidized and reduced species at the same time in contrast to the case of "simple" Ag(II) porphyrins without quinoxaline units where this does not occur. Such an androgynous character of Ag(II) quinoxalinoporphyrins provides new insights into and a rationale for the construction of biomimetic charge-separated and storage ensembles using the same compound acting as both an electron donor and an electron acceptor.

Experimental Section

Chemicals. Absolute dichloromethane (CH_2Cl_2) and pyridine were purchased from Aldrich Co. and used as received without

(7) Kadish, K. M.; E, W.; Ou, Z.; Shao, J.; Sintic, P. J.; Ohkubo, K.; Fukuzumi, S.; Crossley, M. *J. Chem. Soc., Chem. Commun.* **2002**, 356.
(8) Ou, Z.; Kadish, K. M.; E, W.; Shao, J.; Sintic, P. J.; Ohkubo, K.; Fukuzumi, S.; Crossley, M. J. *Inorg. Chem.* **2004**, *43*, 2078.
(9) Harriman, A.; Sauvage, J.-P. *Chem. Soc. Rev.* **1996**, *25*, 41.
(10) (a) Chambron, J. C.; Chardon-Noblat, S.; Harriman, A.; Heitz, V.; Sauvage, J. P. *Pure Appl. Chem.* **1993**, *65*, 2343. (b) Chambron, J.-C.; Collin, J.-P.; Dalbavie, J.-O.; Dietrich-Buchecker, C. O.; Heitz, V.; Odobel, F.; Solladie, N.; Sauvage, J.-P. *Coord. Chem. Rev.* **1998**, *178−180*, 1299.
(11) Blanco, M.-J.; Consuelo Jiménez, M.; Chambron, J.-C.; Heitz, V.; Linke, M.; Sauvage, J.-P. *Chem. Soc. Rev.* **1999**, *28*, 293.
(12) Flamigni, L.; Barigelletti, F.; Armaroli, N.; Collin, J.-P.; Dixon, I. M.; Sauvage, J.-P.; Williams, J. A. G. *Coord. Chem. Rev.* **1999**, *190−192*, 671.
(13) Fukuzumi, S.; Ohkubo, K.; E, W.; Ou, Z.; Shao, J.; Kadish, K. M.; Hutchison, J. A.; Ghiggino, K. P.; Sintic, P. J.; Crossley, M. J. *J. Am. Chem. Soc.* **2003**, *125*, 14984.
(14) Ohkubo, K.; Sintic, P. J.; Tkachenko, N. V.; Lemmetyinen, H.; E, W.; Ou, Z.; Shao, J.; Kadish, K. M.; Crossley, M. J.; Fukuzumi, S. *Chem. Phys.* **2006**, *326*, 3.
(15) Godziela, G. M.; Goff, H. M. *J. Am. Chem. Soc.* **1986**, *108*, 2237.
(16) Kadish, K. M.; Davis, D. G.; Furhop, J.-H. *Angew. Chem., Int. Ed. Engl.* **1972**, *11*, 1014.
(17) Fuhrhop, J.-H.; Kadish, K. M.; Davis, D. G. *J. Am. Chem. Soc.* **1973**, *95*, 5140.
(18) Antipas, A.; Dolphin, D.; Gouterman, M.; Johnson, E. C. *J. Am. Chem. Soc.* **1978**, *100*, 7705.
(19) Karweik, D.; Wigograd, N.; Davis, D. G.; Kadish, K. M. *J. Am. Chem. Soc.* **1974**, *96*, 591.
(20) Scheidt, W. R.; Mondal, J. U.; Eigenbrot, C. W.; Adler, A.; Radonovich, L. J.; Hoard, J. L. *Inorg. Chem.* **1986**, *25*, 795.
(21) For Ag(III) complexes of corroles, see: Brückner, C.; Barta, C. A.; Brinas, R. P.; Krause Bauer, J. A. *Inorg. Chem.* **2003**, *42*, 1673.
(22) For Ag(III) complexes of carbaporphyrins and N-confused porphyrins, see: (a) Furuta, H.; Ogawa, T.; Uwatoko, Y.; Araki, K. *Inorg. Chem.* **1999**, *38*, 2676. (b) Muckey, M. A.; Szczepura, L. F.; Ferrence, G. M.; Lash, T. D. *Inorg. Chem.* **2002**, *41*, 4840.
(23) Wolberg, A.; Manassen, J. *J. Am. Chem. Soc.* **1970**, *92*, 2982.
(24) Fuhrhop, J.-H. *Struct. Bonding* **1974**, *18*, 1.
(25) Scholz, W. F.; Reed, C. A.; Lee, J. L.; Scheidt, W. R.; Lang, G. *J. Am. Chem. Soc.* **1982**, *104*, 6791.
(26) Konishi, S.; Hoshino, M.; Imamura, M. *J. Am. Chem. Soc.* **1982**, *104*, 2057.
(27) For singly oxidized copper(II) phthalocyanine, see: Gardberg, A. S.; Doan, P. E.; Hoffman, B. M.; Ibers, J. A. *Angew. Chem., Int. Ed.* **2001**, *40*, 244.
(28) Erler, B. S.; Scholz, W. F.; Lee, Y. J.; Scheidt, W. R.; Reed, C. A. *J. Am. Chem. Soc.* **1987**, *109*, 2644.
(29) Kadish, K. M.; Lin, X. Q.; Ding, J. Q.; Wu, Y. T.; Araullo, C. *Inorg. Chem.* **1986**, *25*, 3236.
(30) Kadish, K. M.; E, W.; Sintic, P. J.; Ou, Z.; Shao, J.; Ohkubo, K.; Fukuzumi, S.; Govenlock, L. J.; McDonald, J. A.; Try, A. C.; Cai, Z.-L.; Reimers, J. R.; Crossley, M. J. *J. Phys. Chem. B* **2007**, *111*, 8762.
(31) E, W.; Kadish, K. M.; Sintic, P. J.; Khoury, T.; Govenlock, L. J.; Ou, Z.; Shao, J.; Ohkubo, K.; Reimers, J. R.; Fukuzumi, S.; Crossley, M. J. *J. Phys. Chem. A* **2008**, *112*, 556.

Chart 1

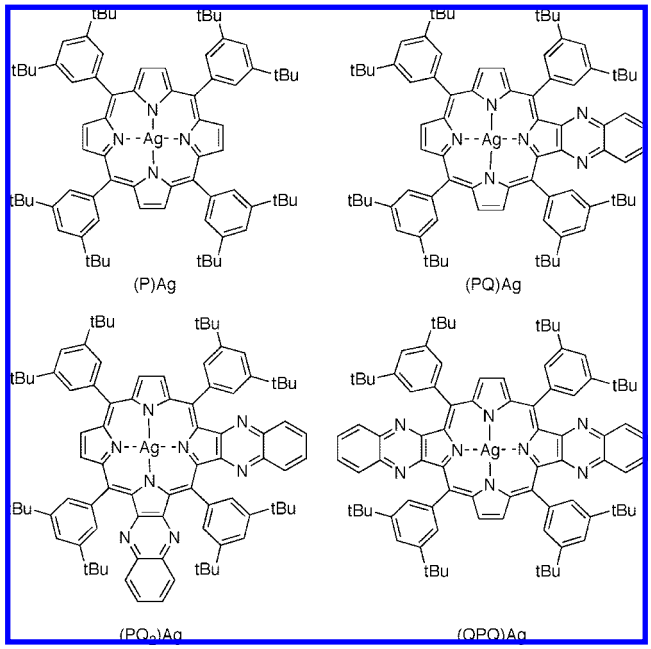

further purification. Benzonitrile (PhCN), obtained from Fluka Chemika Co. or Aldrich Co., was distilled over phosphorus pentaoxide under vacuum before use. Tetra-*n*-butylammonium perchlorate (TBAP) was purchased from Sigma Chemical Co. or Fluka Chemika Co., recrystallized from ethanol, and dried under vacuum at 40 °C for at least one week before use. Tris(2,2′-bipyridyl)-iron(III) hexafluorophosphate, $[Fe(bpy)_3](PF_6)_3$, was prepared by adding 3 equiv of 2,2′-bipyridine to an aqueous solution of ferrous sulfate and then by oxidizing the iron(II) complex with lead dioxide in an aqueous H_2SO_4 solution, followed by the addition of KPF_6.[32]

Electrochemistry. Cyclic voltammograms were obtained with an EG&G Princeton Applied Research (PAR) 173 potentiostat/galvanostat. A homemade three-electrode cell was used and consisted of a platinum button or glassy carbon working electrode, a platinum counter electrode, and a homemade saturated calomel reference electrode (SCE). The SCE was separated from the bulk of the solution by a fritted glass bridge of low porosity that contained the solvent/supporting electrolyte mixture. UV−visible spectroelectrochemical experiments were performed with a home-built thin-layer cell that had a light transparent platinum networking electrode.[33] Potentials were applied and monitored with an EG&G PAR model 173 potentiostat. Time-resolved UV−visible spectra were recorded with a Hewlett-Packard model 8453 diode array spectrophotometer.

General Procedure. Melting points were recorded on a Reichert melting point stage and were uncorrected. Infrared spectra were recorded on an FTIR-8400S Shimadzu Fourier transform infrared spectrophotometer, as solutions in the stated solvents. Intensity abbreviations used are: w, weak; m, medium; s, strong; br, broad. UV−visible spectra were routinely recorded on a Cary 5E UV−vis−NIR spectrophotometer in chloroform that was deacidified by filtration through an alumina column. High-resolution electrospray ionization Fourier transform ion cyclotron resonance (HR-ESI-FT/ICR) spectra were acquired at the Research School of Chemistry, Australian National University, on a Bruker Daltonics BioAPEX II FT/ICR mass spectrometer equipped with a 4.7 T MAGNEX superconducting magnet and an analytical external ESI source. Column chromatography was routinely carried out using the gravity feed column technique on Merck silica gel type 9385 (230−400 mesh). Analytical thin-layer chromatography (TLC) analyses were performed on Merck silica gel 60 F254 precoated sheets (0.2 mm). All commercial solvents were routinely distilled before use. Light petroleum refers to the fraction of bp 60−80 °C. Ethanol-free chloroform was obtained by drying distilled chloroform over calcium chloride and passing it through a column of alumina immediately before use. Where solvent mixtures were used, the proportions are given by volume.

Synthesis. The silver(II) porphyrins were prepared in high yield from their corresponding free-base analogues[34] by treatment with silver(II) acetate. IR and UV−vis spectra showed patterns consistent with metal(II) porphyrins, and high-resolution mass spectra analysis confirmed the molecular formula of each complex. The detail for synthesis and analytical data are shown in Supporting Information S1−S3.

EPR Measurements. EPR spectra of silver(II) porphyrins were recorded on a JEOL JES-RE1XE spectrometer. The singly oxidized products were produced by a one-electron oxidation of the silver(II) porphyrins with $[Fe(bpy)_3]^{3+}$ (bpy = 2,2′-bipyridine) in CH_2Cl_2.[32] EPR spectra of the singly oxidized species were measured at 298 and 77 K. The magnitude of modulation was chosen to optimize the resolution and signal-to-noise (S/N) ratio of the observed spectra under nonsaturating microwave power conditions. The *g* values and hyperfine coupling constants were calibrated using an Mn^{2+} marker.

Calculations. Theoretical calculations of the properties of molecules were performed using density functional theory (DFT) with the B3LYP density functional[35] and the 3-21G* basis set. All calculations were performed using Gaussian 03.[36] Graphical outputs of the computational results were generated with the Gauss View software program (version 3.09) developed by Semichem, Inc.[37]

Laser Flash Photolysis Measurements. Measurements of nanosecond transient absorption spectrum were performed according to the following procedure. The laser system was provided by UNISOKU Co., Ltd. A deaerated PhCN solution containing the silver porphyrin and photosensitizer [(P)Zn or tetramethyl-*p*-benzoquinone] was excited by Nd:YAG laser (Continuum, SLII-10, 4−6 ns fwhm) with 10−30 mJ/pulse. Time courses of the transient absorption spectra were measured by using a continuous Xe lamp (150 W) and an In GaAs-PIN photodiode (Hamamatsu 2949) as a probe light and a detector, respectively. The output from the photodiodes and a photomultiplier tube was recorded with a digitizing oscilloscope (Tektronix, TDS3032, 300 MHz). The transient spectra were recorded using fresh solutions in each laser excitation. All experiments were performed at 298 K. The solution was deoxygenated by argon purging for 15 min before the measurements.

Results and Discussion

EPR Spectra of Silver(II) Porphyrins. The EPR spectra of {5,10,15,20-tetrakis(3,5-di-*tert*-butylphenyl)porphyrinato}silver(II) [(P)Ag] and {5,10,15,20-tetrakis(3,5-di-*tert*-butylphenyl)quinoxalino[2,3-*b*′]porphyrinato}silver(II) [(PQ)Ag] in CH_2Cl_2 are shown in Figure 1a,c together with the computer simulation spectra in Figure 1b,d. The hyperfine splitting patterns due to the Ag nuclei (I = 1/2) and four equivalent nitrogens, each of which has I = 1, are virtually the same as earlier reported for Ag(II) porphyrins with other macrocyles.[38–40]

(32) Fukuzumi, S.; Nakanishi, I.; Tanaka, K.; Suenobu, T.; Tabard, A.; Guilard, R.; Van Caemelbecke, E.; Kadish, K. M. *J. Am. Chem. Soc.* **1999**, *121*, 785.
(33) Lin, X. Q.; Kadish, K. M. *Anal. Chem.* **1985**, 1489.
(34) Crossley, M. J.; Sintic, P. J.; Walton, R.; Reimers, J. R. *Org. Biomol. Chem.* **2003**, *1*, 2777–2787.
(35) Becke, A. D. *J. Chem. Phys.* **1993**, *98*, 5648.
(36) Frisch, M. J.; et al. *Gaussian 03*, revision C.02; Gaussian, Inc.: Wallingford, CT, 2004. For full list of authors, see Supporting Information S9.
(37) Dennington, R., II; Keith, T.; Millam, J.; Eppinnett, K.; Hovell, W. L.; Gilliland, R. *Gaussview*; Semichem: Shawnee Mission, KS, 2003.
(38) Kneubühl, F. K.; Koski, W. S.; Caughey, W. S. *J. Am. Chem. Soc.* **1961**, *83*, 1607.

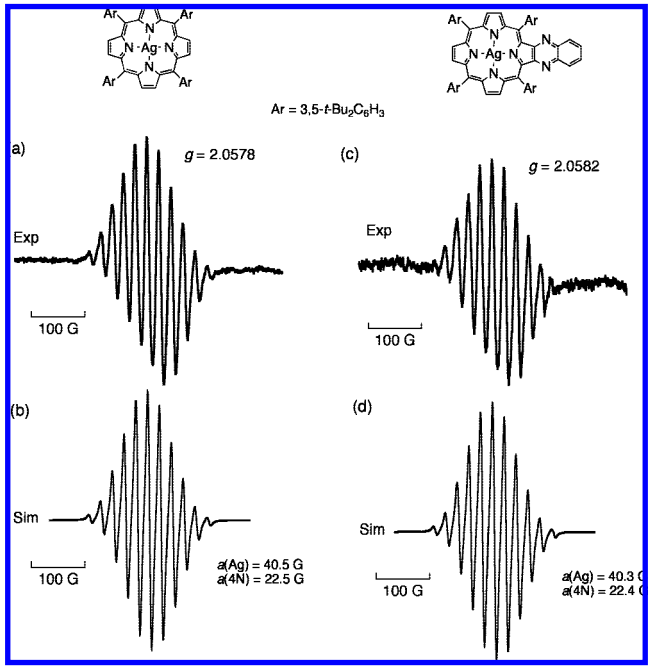

Figure 1. EPR spectra of (a) (P)Ag and (c) (PQ)Ag in CH_2Cl_2. The computer simulation spectra are given with a(Ag) and a(4N) values in (b) and (d), respectively.

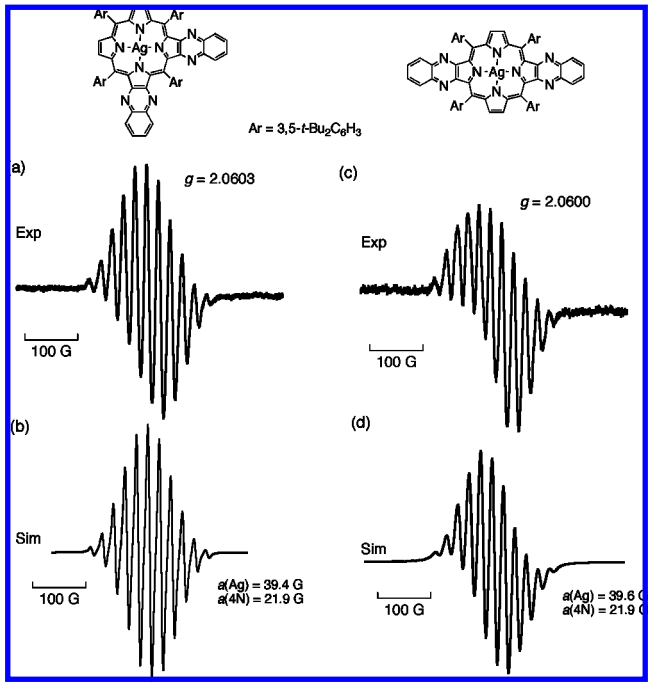

Figure 2. EPR spectra of (a) (PQ_2)Ag and (c) (QPQ)Ag in CH_2Cl_2. The computer simulation spectra are given with a(Ag) and a(4N) values in (b) and (d), respectively.

The a(Ag) and a(4N) values of (PQ)Ag are also identical within experimental error to those of (P)Ag.

Figure 2 shows the EPR spectra of {5,10,15,20-tetrakis(3,5-di-*tert*-butylphenyl)bisquinoxalino[2,3-*b*′:7,8-*b*″]porphyrinato}silver(II)[(PQ_2)Ag] and {5,10,15,20-tetrakis(3,5-di-*tert*-butylphenyl)bisquinoxalino[2,3-*b*′:12,13-*b*″]porphyrinato}silver(II) [(QPQ)Ag] in CH_2Cl_2 along with the computer simulation spectra of the two compounds. The a(Ag) and a(4N) values of the two bisquinoxalinoporphyrins, (PQ_2)Ag and (QPQ)Ag, are slightly smaller than those of the parent compound (P)Ag and the monoquinoxaline derivative (PQ)Ag. The EPR results in Figures 1 and 2 are well-explained by the DFT calculations.

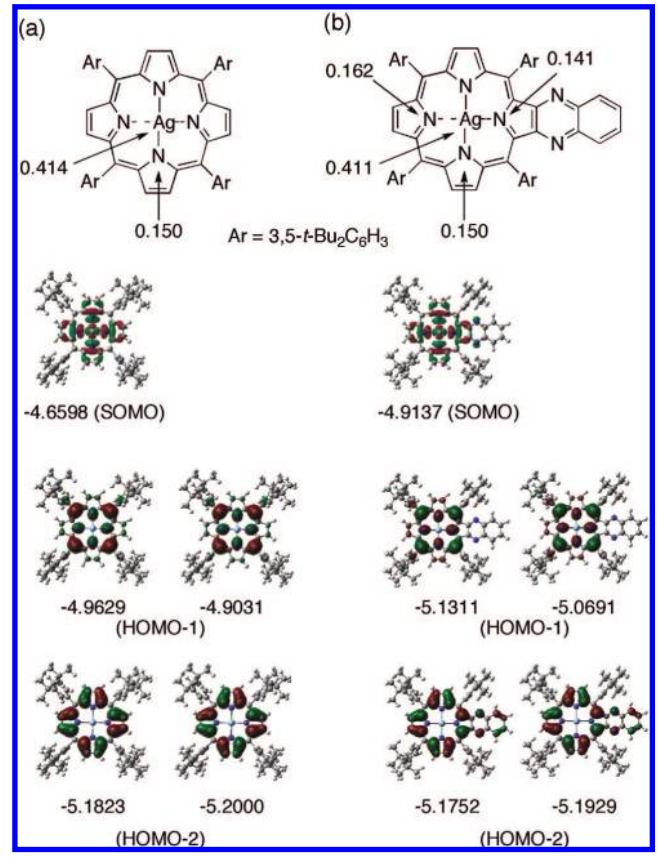

Figure 3. Calculated spin densities and frontier molecular orbitals with α (left) and β (right) spins of (a) (P)Ag and (b) (PQ)Ag (energy is given in electronvolts).

Figure 3 shows the SOMO of (P)Ag and (PQ)Ag with the spin densities [top columns of (a) and (b), respectively] together with the lower occupied orbitals of α and β spins (see Experimental Section for calculation method). The calculated spin densities on the Ag and pyrrole nitrogens are virtually the same for (P)Ag and (PQ)Ag, where 41% of the spin is on the Ag(II) ion. The SOMO in each case involves the metal-centered orbital. The HOMO−1 is solely a macrocycle-centered orbital (a_{1u} type orbital) and is significantly lower in energy than the SOMO. This suggests that the first electron-transfer oxidation of (P)Ag and (PQ)Ag should occur at the metal center and the second at the porphyrin π-ring system, and this is exactly what is observed as discussed in later sections of this article.

Figure 4 shows the calculated spin densities for the frontier molecular orbitals of (PQ_2)Ag and (QPQ)Ag. The unoccupied molecular orbitals are given in Supporting Information S4. The calculated spin densities on the Ag and pyrrole nitrogens of (PQ_2)Ag and (QPQ)Ag are slightly smaller than those of (P)Ag and (PQ)Ag (see EPR spectra in Figure 2). In contrast to the case of (P)Ag and (PQ)Ag (Figure 3), the SOMO energy involving the metal-centered orbitals of (PQ_2)Ag and (QPQ)Ag are quite close to the HOMO−1 (a_{1u}) energy of the macrocycle-

(39) MacCragh, A.; Storm, C. B.; Koski, W. S. *J. Am. Chem. Soc.* **1965**, *87*, 1470.
(40) Brown, T. G.; Hoffman, B. M. *Mol. Phys.* **1980**, *39*, 1073.

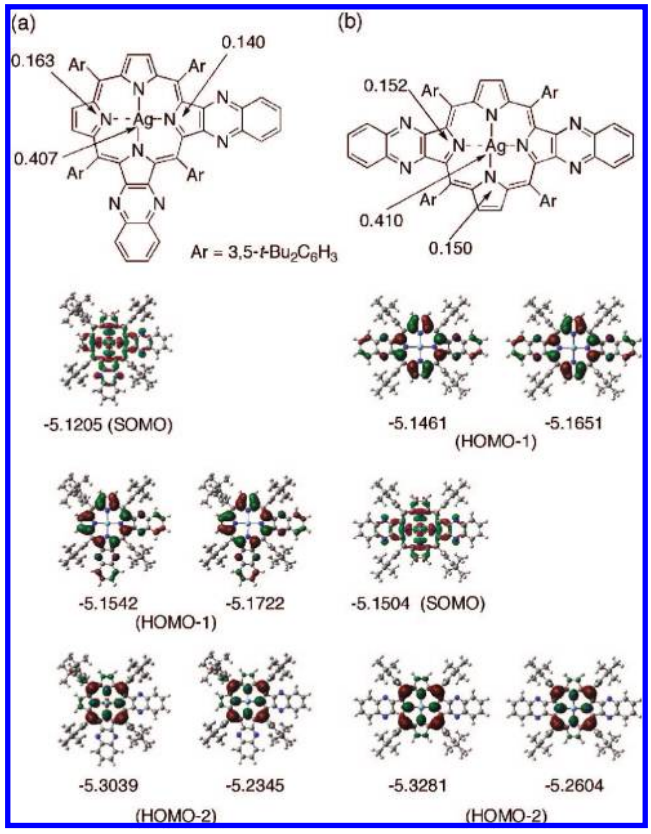

Figure 4. Calculated spin densities and frontier molecular orbitals with α (right) and β (left) spins of (a) $(PQ_2)Ag$ and (b) (QPQ)Ag (energy is given in electronvolts).

centered orbital. It should be noted that the ordering of the a_{1u}- and a_{2u}-type orbitals changes with increasing substitution. The actual site of electron transfer in each redox reaction of (P)Ag, (PQ)Ag, $(PQ_2)Ag$, and (QPQ)Ag was examined experimentally by electrochemistry, UV−vis spectroelectrochemistry, and EPR spectroscopy (vide infra), and this is discussed in the following sections.

Electrochemistry of Silver(II) Porphyrins. Figure 5 compares cyclic voltammograms for the oxidation and reduction of the investigated compounds in pyridine. As seen in the figure, each Ag(II) porphyrin undergoes one oxidation and two reductions within the potential range of the pyridine solvent.[41,42] The addition of one or two quinoxaline groups to the porphyrin macrocycle results in a positive shift of all potentials as compared to oxidation or reduction of the parent (P)Ag compound. The magnitude of the potential shift upon adding one or two fused quinoxaline groups to the macrocycle is much larger for reductions than that for oxidations as seen, for example, by a comparison of (P)Ag and (QPQ)Ag in pyridine. The (P)Ag undergoes a one-electron reduction and one-electron oxidation at −0.94 and +0.64 V, while the linear bisquinoxaline derivative is reduced and oxidized at −0.60 and +0.81 V under the same solution conditions. Thus, the one-electron oxidation of (P)Ag (E_{ox}) is easier by 170 mV than the Ag(II)/Ag(III)

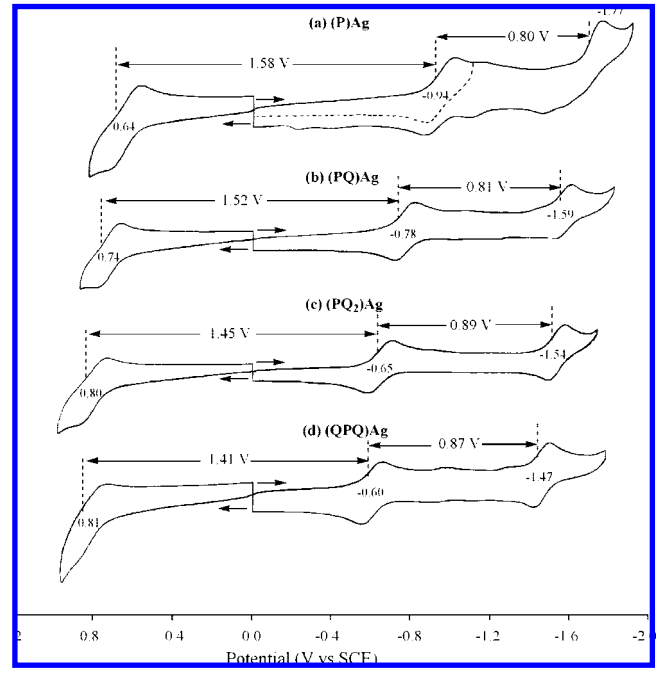

Figure 5. Cyclic voltammograms of (a) (P)Ag, (b) (PQ)Ag, (c) $(PQ_2)Ag$, and (d) (QPQ)Ag in pyridine, 0.1 M TBAP.

process of (QPQ)Ag and the one-electron reduction of (P)Ag (E_{red}) is harder by 340 mV than the reversible Ag(II)/Ag(I) process of (QPQ)Ag.

As shown in Figures 3 and 4, the SOMO energy decreases with increased delocalization on the porphyrin ligand orbital. The decrease in energy follows the order: (P)Ag < (PQ)Ag < $(PQ_2)Ag$ < (QPQ)Ag, and this parallels the positive potential shift in the first reduction of the compounds as illustrated in Figure 5. Such a trend was earlier reported for other metalated quinoxalinoporphyrins with electroinactive metal ions.[30,31,43]

With regard to the oxidation, the first electron is removed from the SOMO, and the E_{ox} value is shifted in a positive direction with decreasing SOMO energy, as also occurs for E_{red}. The SOMO energy decreases with increasing delocalization at the porphyrin ligand orbital. The smaller degree of solvation due to delocalization results in a positive shift of the redox potentials. The more significant change in E_{red} values as compared to E_{ox} upon introduction of one or two quinoxaline moieties onto the porphyrin ring suggests that solvation has a less pronounced effect on the oxidation as compared to the case of the reduction.

Redox potentials were also measured in the nonbonding solvent CH_2Cl_2. The solvent window for observing oxidations is much extended over that of pyridine and two oxidations could be observed, but the reductions are ill-defined in this solvent and were not further investigated in CH_2Cl_2 because of the presence of coupled chemical reactions and demetalation of the electrogenerated Ag(I) in the absence of a coordinating solvent.[29]

Cyclic voltammograms illustrating the two reversible oxidations in CH_2Cl_2 are given in Figure 6, and the measured half-

(41) The reduction wave of free base H2P is also seen because of partial demetalation associated with the reduction of (P)Ag at−1.1 V in Figure 5a; see refs[43] and.[44] For photoinduced demetalation of (TPP)Ag under reducing conditions, see: Kunkely, H.; Vogler, A. *Inorg. Chem. Commun.* **2007**, *10*, 479.

(42) Giraudeau, A.; Louati, A.; Callot, H. J.; Gross, M. *Inorg. Chem.* **1981**, *20*, 769.

(43) (a) Ou, Z.; E, W.; Shao, J.; Burn, P. L.; Sheehan, C. S.; Walton, R.; Kadish, K. M.; Crossley, M. J. *J. Porphyrins Phthalocyanines* **2005**, *9*, 142. (b) Sintic, P. J.; E, W.; Ou, Z.; Shao, J.; McDonald, J. A.; Cai, Z.; Kadish, K. M.; Crossley, M. J.; Reimers, J. R. *Phys. Chem. Chem. Phys.* **2008**, *10*, 515. (c) Ou, Z.; E, W.; Zhu, W.; Thordarson, P.; Sintic, P. J.; Crossley, M. J.; Kadish, K. M. *Inorg, Chem.* **2007**, *46*, 10840.

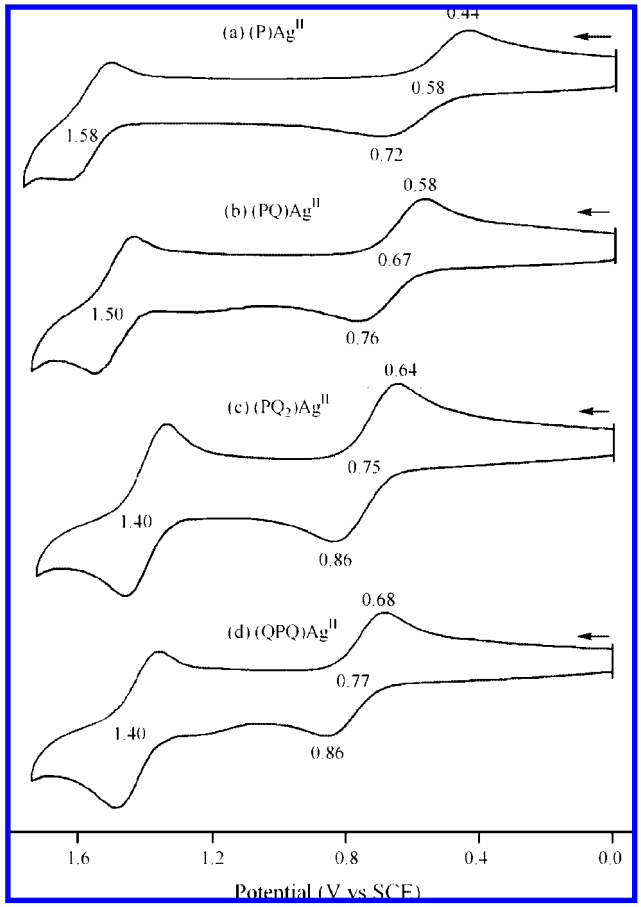

Figure 6. Cyclic voltammograms of (a) (P)Ag, (b) (PQ)Ag, (c) (PQ_2)Ag, and (d) (QPQ)Ag in CH_2Cl_2, 0.1 M TBAP.

Table 1. Half-Wave Potentials (V vs SCE) for Oxidation and Reduction of Silver(II) Porphyrins in Pyridine and CH_2Cl_2 Containing 0.1 M TBAP

solvent	macrocycle	2nd ox	1st ox	1st red	2nd red
pyridine	P	*a*	0.64	−0.94	−1.77[b]
	PQ	*a*	0.74	−0.78	−1.59
	PQ_2	*a*	0.80	−0.65	−1.47
	QPQ	*a*	0.81	−0.60	−1.54
CH_2Cl_2	P	1.58	0.58	*c*	*c*
	PQ	1.50	0.67	*c*	*c*
	PQ_2	1.40	0.75	*c*	*c*
	QPQ	1.40	0.77	*c*	*c*

[a] Reaction occurred beyond the positive potential limit of the solvent. [b] Peak potential measured at a sweep rate of 0.10 V/s. [c] Reactions ill-defined because of coupled chemical reactions and demetalation in this solvent.

wave potentials in both solvents are summarized in Table 1. The potentials for the first one-electron oxidation are similar in the bonding and nonbonding solvents although the reactions are slightly easier in CH_2Cl_2 because of a stronger ion-pairing interaction of the electrogenerated Ag(III) porphyrins with the perchlorate anion from the supporting electrolyte. It should also be pointed out that potentials for the second one-electron oxidation are shifted in a negative direction with an increase in the number of fused quinoxaline groups on the molecule as compared to a positive shift in $E_{1/2}$ for the first reduction process (Figure 6). The negative potential shift in the second oxidation was not observed for previously investigated M(II) quinoxalinoporphyrins[31] and leads to a decrease in the potential separation between the two oxidations from 1.00 V in the case of (P)Ag

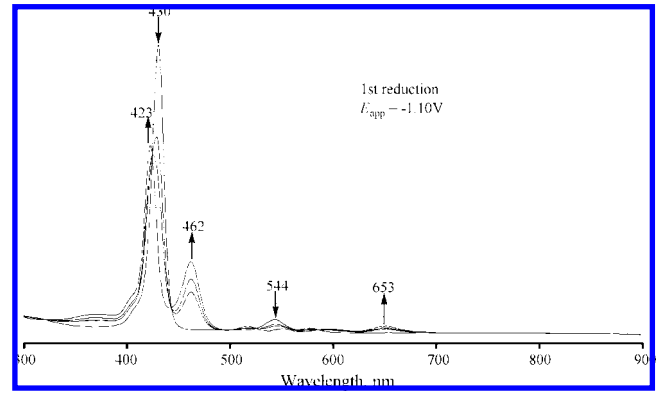

Figure 7. Thin-layer UV−visible spectral changes during the Ag(II)/Ag(I) process in pyridine containing 0.1 M TBAP for (P)Ag at a controlled potential of −1.10 V vs SCE.

to 0.83 V for (PQ)Ag and then to 0.63−0.65 V for (PQ_2)Ag and (QPQ)Ag. This trend is consistent with the electrogenerated porphyrin radical cation being stabilized by extended π-delocalization because of the quinoxaline moieties as indicated by the SOMO−1 in Figures 3 and 4, and this is facilitated by a strong association of the doubly oxidized porphyrin with the perchlorate anion of the supporting electrolyte.

Site of Electron Transfer in Silver(II) Porphyrins. The site of electron transfer after oxidation or reduction of a given metalloporphyrin can in many cases be identified by measuring UV−vis spectra of the electrogenerated products.[2] In the current study, the spectral changes were in almost all cases reversible upon electrooxidation or electroreduction, and an example of these changes is shown in Figure 7 for the electroreduction of (P)Ag in a thin-layer cell containing pyridine, 0.1 M TBAP. As seen from the figure, the sharp Soret band due to (P)Ag^{II} at 430 nm and the Q-band at 544 nm both disappear as the Ag(I) form of the compound is generated. The singly reduced porphyrin has a split Soret band with decreased intensity at λ = 423 and 462 nm and a Q-band at 653 nm. The electron addition to (P)Ag is reversible on the spectroelectrochemical time scale, and the original spectrum of the unreduced porphyrin could be obtained by application of a positive applied potential to regenerate the starting compound. Similar spectral changes were reported earlier for the electrochemical reduction of (TPP)Ag^{II} to give [(TPP)Ag^{I}]$^-$ in DMSO.[29]

Although the observed spectral changes for the first one-electron reduction of (P)Ag are reversible in pyridine, the second electron addition is not reversible, presumably due to demetalation of Ag^{I} as described in the literature[29] for [(TPP)Ag^{I}]$^-$ and its phenyl-substituted derivatives. In contrast, a demetalation is not observed after the first or second reductions of the investigated quinoxalinoporphyrins in pyridine on the spectroelectrochemical time scale, and this is documented by the reversible current−voltage curves in Figure 5.

Thus, a fusion of one or two quinoxaline groups to the porphyrin giving PQ, QPQ, and PQ_2 leads not only to easier reductions but also to an enhanced stability of the singly and doubly reduced species which are assigned, respectively, to an Ag(I) porphyrin in the first electron addition and then to an Ag(I) porphyrin π-anion radical in the second. The absolute potential separation between these two processes ranges from 0.80 to 0.89 V (Figure 5) and is as expected based on similar assignments of electron transfer site in a large number of iron and cobalt porphyrins,[2] the most well-studied of which are (TPP)Fe and (TPP)Co.

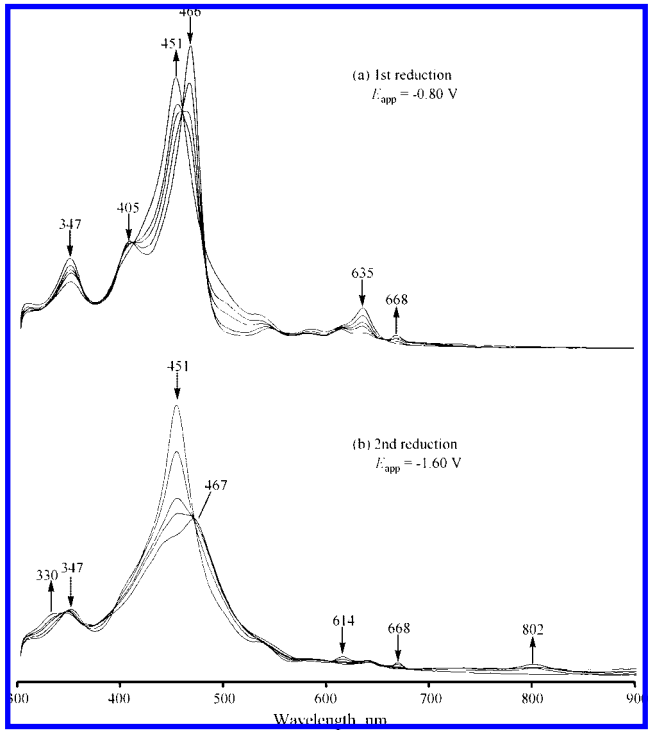

Figure 8. Thin-layer UV−vis spectral changes of (QPQ)Ag in pyridine, 0.2 M TBAP during potential reduction (a) at −0.80 V vs SCE to give an Ag(I) porphyrin and (b) during the following porphyrin ring-centered reduction at −1.60 V vs SCE.

The enhanced stability of the electroreduced quinoxalinoporphyrins enabled measurements of their UV−vis spectra in a thin-layer cell and examples of the spectral changes which occurred during electron transfer for (QPQ)Ag in pyridine are given in Figure 8a,b. During the first reduction, the Soret band of (QPQ)Ag is shifted from 466 to 451 nm, while the Q-band absorptions at 635 nm for the neutral compound disappear as a new band grows in at 668 nm (Figure 8a). No loss of Soret band intensity occurs after the first one-electron reduction of (QPQ)Ag, but this is not the case after the second electron addition at an applied potential of −1.60 V. This spectrum is illustrated in Figure 8b and is diagnostic for formation of a porphyrin π-radical anion in that it possesses a much decreased Soret band intensity and broad absorption band in the long wavelength region of the spectrum.

The spectra of singly and doubly reduced (PQ)Ag and (PQ_2)Ag were also electrogenerated in a thin-layer cell. The spectral changes under application of an appropriate applied reducing potential in pyridine are shown in Figures S5 and S6, respectively.

The first and second one-electron oxidations of all four compounds are also reversible in CH_2Cl_2 (Figure 6). An example of the resulting spectral changes during the Ag(II)/Ag(III) process and further oxidation to give the Ag(III) π-cation radical is shown in Figure 9 for the case of (PQ)Ag in CH_2Cl_2, 0.1 M TBAP.

The first one-electron abstraction from (PQ)Ag leads to a shift in wavelength maxima for the Soret and Q bands of the compound, but there is not a big change in intensity of the bands as the Ag(III) form of the porphyrin is generated in solution. This is expected for an M(II)/M(III) process of the porphyrin and contrasts with what would be observed during formation of a porphyrin π-cation radical where the spectrum of the singly

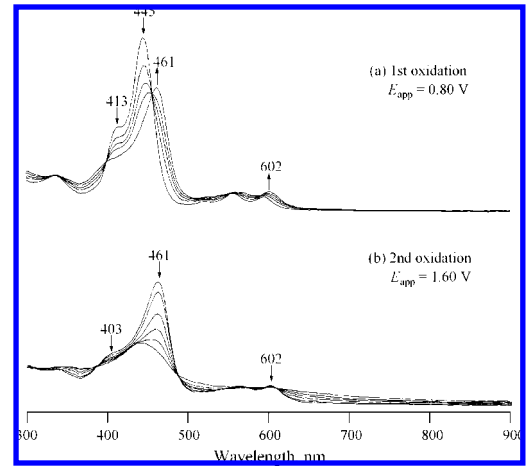

Figure 9. Thin-layer UV−vis spectral changes during controlled potential oxidation of (PQ)Ag in CH_2Cl_2 containing 0.1 M TBAP at (a) 0.80 and (b) 1.60 V.

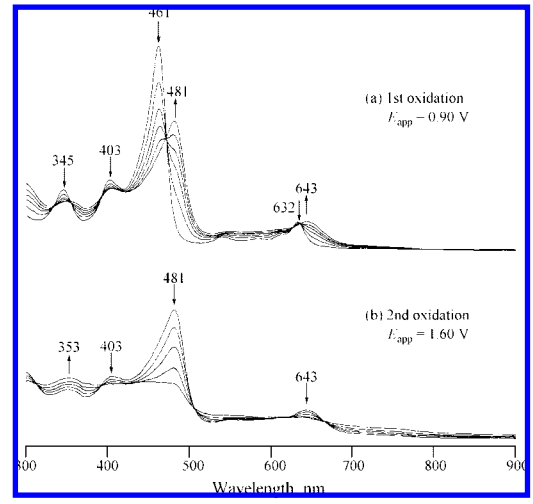

Figure 10. Thin-layer UV−vis spectral changes in CH_2Cl_2 containing 0.1 M TBAP for (QPQ)Ag during the oxidation process at a controlled potential of (a) 0.90 and (b) 1.60 V.

oxidized species should have Soret and Q bands which are both significantly decreased in intensity. The π-cation radical spectrum should also possess a diagnostic broad absorption band in the long wavelength region of the spectrum; this is exactly what is observed after the second oxidation of (PQ)Ag, as shown in Figure 9b.

UV−vis spectra for the singly and doubly oxidized forms of (QPQ)Ag and (PQ_2)Ag in CH_2Cl_2 were also obtained, and these spectra are shown in Figures 10 and S7. The first one-electron oxidation occurs at the central metal to generate the Ag(III) form of the porphyrin. These reactions are observed for all four investigated porphyrins, irrespective of the increased porphyrin π-extension upon going from P to PQ and then to PQ_2 or QPQ. It should be noted that no triplet EPR signal is observed at 77 K for the singly oxidized (PQ_2)Ag or (QPQ)Ag which are produced after a one-electron oxidation with $[Fe(bpy)_3]^{3+}$ (bpy = 2,2′-bipyridine) (Supporting Information S8).[44]

Androgynous Characteristics of (QPQ)Ag. The small HOMO−LUMO gap of (QPQ)Ag (Figure 5) makes it possible for (QPQ)Ag to act as both an electron donor and an electron acceptor in photoinduced electron-transfer reactions. This is exemplified in the photoinduced electron transfer from (QPQ)Ag

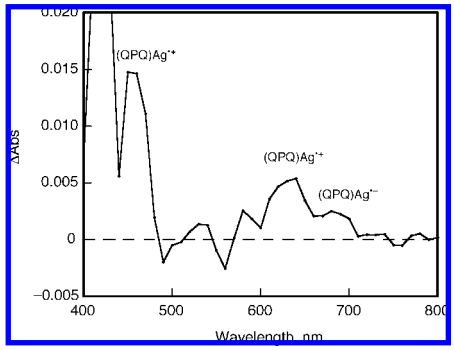

Figure 11. Transient absorption spectrum of (QPQ)Ag (3.0×10^{-4} M) with (P)Zn (2.0×10^{-5} M) obtained by nanosecond laser flash photolysis in deaerated PhCN at 298 K at 300 μs after laser excitation ($\lambda = 440$ nm).

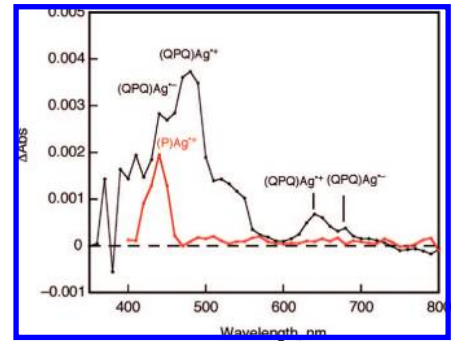

Figure 12. Transient absorption spectra of (QPQ)Ag (3.0×10^{-4} M; black line) and (P)Ag (3.0×10^{-4} M; red line) with tetramethyl-*p*-benzoquinone (2.5×10^{-3} M) obtained by nanosecond laser flash photolysis in deaerated PhCN at 298 K at 1.0 ms after laser excitation ($\lambda = 355$ nm).

to the triplet excited state of {5,10,15,20-tetrakis(3,5-di-*tert*-butylphenyl)porphyrinato}zinc, ^{3}[(P)Zn]*. The photoexcitation of a deaerated PhCN solution (P)Zn and (QPQ)Ag affords both $([QPQ]Ag)^+$ ($\lambda_{max} = 481$ and 643 nm, cf. Figure 10) and $[(QPQ)Ag]^-$ ($\lambda_{max} = 451$ and 668 nm, cf. Figure 8) as shown in Figure 11. The one-electron reduced species $[(QPQ)Ag]^-$ is formed by photoinduced electron transfer from ^{3}[(P)Zn]* ($E_{ox} = -0.81$ V vs SCE)[45] to (QPQ)Ag ($E_{red} = -0.60$ V vs SCE), whereas the one-electron oxidized species $[QPQ)Ag]^+$ is formed by subsequent electron transfer from (QPQ)Ag ($E_{ox} = 0.77$ V vs SCE) to $[(P)Zn]^{\bullet+}$ ($E_{red} = 0.77$ V vs SCE) in PhCN.[43a,46] Although the driving force of electron transfer from (QPQ)Ag to $[(P)Zn]^{\bullet+}$ is zero, the large excess of (QPQ)Ag relative to $[(P)Zn]^{\bullet+}$ results in completion of the electron-transfer reaction. In contrast, the photoexcitation of a deaerated solution of (P)Zn and (P)Ag affords only ^{3}[(P)Zn]*, and neither electron transfer from ^{3}[(P)Zn]* to (P)Ag nor from (P)Ag to ^{3}[(P)Zn]* occurred, because both electron-transfer processes are thermodynamically infeasible.

The photoexcitation of a deaerated PhCN solution of Me_4Q and (QPQ)Ag also affords both $[(QPQ)Ag]^+$ and $[(QPQ)Ag]^-$ as shown in Figure 12. In contrast, the photoexcitation of a deaerated solution of Me_4Q and (P)Ag affords only $[(P)Ag]^+$ ($\lambda_{max} = 440$ nm) (red line in Figure 12). In this case, the absorption band due to $Me_4Q^{\bullet-}$ ($\lambda_{max} = 450$ nm) is overlapped with the band due to $[(P)Ag]^+$. In both cases, photoinduced electron transfer from (QPQ)Ag and (P)Ag to the triplet excited state of Me_4Q occurs efficiently to produce the oxidized species ($[(QPQ)Ag]^+$ and $[(P)Ag]^+$) and the reduced species ($Me_4Q^{\bullet-}$). In the case of (P)Ag, electron transfer from $Me_4Q^{\bullet-}$ ($E_{ox} = -0.85$ V vs SCE)[47] to (P)Ag ($E_{red} = -0.94$ V vs SCE) is endergonic, and thereby $[(P)Ag]^-$ cannot be formed. In contrast, electron transfer from $Me_4Q^{\bullet-}$ to (QPQ)Ag ($E_{red} = -0.60$ V vs SCE) is thermodynamically allowed to occur to produce $[(QPQ)Ag]^-$. Thus, (QPQ)Ag indeed has an androgynous character by being able to act as both a good electron donor and a good electron acceptor. Such a unique androgynous character of (QPQ)Ag opens new opportunities to use the same compound as both an electron donor and an electron acceptor moiety in charge-separation ensembles.

Acknowledgment. This work was partially supported by a Grant-in-Aid (No. 19205019) and a Global COE program, "the Global Education and Research Center for Bio-Environmental Chemistry" from the Ministry of Education, Culture, Sports, Science and Technology, Japan. The support of the Robert A. Welch Foundation (K.M.K., Grant E-680) and the Texas Advanced Research program (K.M.K., Grant No. 003652-0018-2001) is also gratefully acknowledged. This work was also partially supported by a Discovery Research Grant (DP0208776) to M.J.C. from the Australian Research Council.

Supporting Information Available: Details of synthesis and analytical data (S1−S3), unoccupied molecular orbitals of $(PQ_2)Ag$ and (QPQ)Ag (S4), spectroelectrochemical data (S5−S7), and EPR data (S8). Full list of authors for ref 36 (S9). This material is available free of charge via the Internet at http://pubs.acs.org.

JA801318B

(44) For the formation of a triplet in silver(II) porphyrins in the solid state, see: Marumoto, K.; Takahashi, H.; Tanaka, H.; Kuroda, S.; Ishii, T.; Kanehama, R.; Aizawa, N.; Yamashita, M. *J. Phys.: Condens. Matter* **2004**, *16*, 8753.

(45) Imahori, H.; Tamaki, K.; Guldi, D. M.; Luo, C.; Fujitsuka, M.; Ito, O.; Sakata, Y.; Fukuzumi, S. *J. Am. Chem. Soc.* **2001**, *123*, 2607.

(46) Although the free energy change of electron transfer from (QPQ)Ag to $[(P)Zn]^{\bullet+}$ is zero, the much larger concentration of (QPQ)Ag as compared to that of $[(P)Zn]^{\bullet+}$ allows the electron transfer to undergo completion.

(47) Fukuzumi, S.; Nishizawa, N.; Tanaka, T. *J. Org. Chem.* **1984**, *49*, 3571.